

BROWNIAN MOTION IN POTENTIAL WELLS: THE EFFECT OF EXTERNAL  
ELECTRIC FIELDS

M.W. EVANS, F. MARCHESONI and S.J. ABAS

Department of Physics, U.C.N.W., Bangor, Gwynedd, Wales.  
Department of Theoretical Physics, D.I.A.S., 10 Burlington Road,  
Dublin, Ireland.  
Department of Applied Mathematics, U.C.N.W., Bangor, Gwynedd,  
Wales.

(Received 21 September 1985)

ABSTRACT

The theory of Brownian motion in cosinal potential wells produces numerous resonance peaks in the far infra-red power absorption coefficient when the friction coefficient ( $\beta$ ) becomes small. The same rotational Langevin equation produces a dielectric loss  $\epsilon''(\omega)$  at lower frequencies resembling the bell-shaped curve of Debye. This shape is also recovered from the less well-known Ivanov jump model, valid, as for Debye, at low frequencies only. In this letter, we explore formally the effect of using a "complex friction" coefficient of the form  $(\beta - i\omega)$  to describe the cross-mode coupling induced by an electric field. It is found that as  $\omega$  is increased the dielectric loss sharpens, shifts, and broadens in cycles, and fine structure is periodically resolved on the high frequency side. The peaks in the far infra-red power absorption coefficient shift in relative intensity and position in an intricate pattern. An interpretation of "complex friction" is given in terms of two linked Langevin equations, for rototranslational Brownian motion in a pseudo-potential well that is periodic in the two dynamical variables that appear in the equations.

INTRODUCTION

The theory of Brownian motion in potential wells has been given a new impetus recently by Reid [1], who provided the first complete numerical solution of the Kramers equation [2]:

$$\frac{\partial \rho}{\partial t} + \dot{\theta} \frac{\partial \rho}{\partial \theta} - \frac{V'}{I} \frac{\partial \rho}{\partial \dot{\theta}} = \beta \frac{\partial}{\partial \dot{\theta}} \left[ \dot{\theta} \rho + \frac{kT}{I} \frac{\partial \rho}{\partial \dot{\theta}} \right] \quad (1)$$

$$V = -V_0 \cos N\theta .$$

Here  $\rho(\theta, \dot{\theta}, t | \theta(0), \dot{\theta}(0), 0)$  is the phase space joint conditional probability density function governing the time dependence of  $\theta$ , an angular coordinate describing molecular rotational motion constrained to two dimensions for simplicity of argument - the so-called "circular diffusion" process. The rotational motion takes place in potential wells of the type (2), where  $V_0$  is the barrier height and  $N$  the well multiplicity.  $I$  is the effective molecular moment of inertia and  $\beta$  the friction coefficient of the equivalent rotational Langevin equation [3]:

$$I\ddot{\theta} + I\beta\dot{\theta} + V'(\theta) = \dot{W}(t) \quad (2)$$

where  $\dot{W}(t)$  is a Wiener process. The parameter  $\beta$  can also be interpreted as the frequency of escape from the potential wells, or barrier jumping frequency. Equation (3) therefore effectively combines the concepts of diffusion [3] (Debye) and well jumping [4] (Ivanov), and includes the inertial term  $I\ddot{\theta}$ . Equations of the form (2) and (3) are also of use in the description of  $V-I$  characteristics in Josephson junction hysteresis [5], and for a range of other phenomena [6], including ionic diffusion and super-conductivity. Reid's results are given in terms of the parameters [1]:

$$\alpha = (kT/I)^{1/2} ; \quad \beta ; \quad \text{and} \quad \gamma = V_0/(2IkT)^{1/2}$$

The numerical solution of equation (1) leads to the appearance of fine structure in the far infra-red power absorption coefficient  $\alpha(\omega)$  and to a broad, low frequency dielectric loss ( $\epsilon''(\omega)$ ) curve with the additional structure superimposed at high frequencies. Here  $\omega$  is the angular frequency in radians  $\text{sec}^{-1}$ . Experimental evidence for this type of fine structure is available [7] for fluid acetonitrile and in liquid crystals subjected to

external electric fields [8]. In these experimental papers the effect of a static, external electric field on the far infra-red structure is reported to be to shift the individual peaks in position and intensity.

In this paper we initiate the formal development of the theory (equation (1)) in order to consider the effect on  $\alpha(\omega)$  and  $\epsilon''(\omega)$  of an extra field term. The way this is done depends on the nature of the field. The external, static, electric field may be incorporated by rewriting equation (1) as:

$$I\ddot{\theta} + I\dot{\theta} + V'_1(\theta) = \dot{W}(t) \quad (3)$$

$$V_1(\theta) = -V_0 \cos N(\theta) - \mu E \cos(\theta - \theta_0)$$

where  $\mu$  is the molecular dipole moment and  $E$  the electric field strength (volts  $\text{cm}^{-1}$ ). In this case the electric field effectively produces an increase in the parameter  $\gamma$ , for constant  $\alpha, \beta$ , and  $N$ . It is clear from the structure of equation (3) that the extra term  $\mu E \sin \theta$  will produce more peaks in the far infra-red, because of the new librational frequency proportional to  $E$ .

If the angular velocity variable  $\dot{\theta}$  is correlated with another dynamical variable in the system under consideration, for example the linear molecular centre of mass velocity  $\underline{v}$ , then it is well known that the dynamics of the molecular ensemble can be described with equations of the type (3), but with  $\dot{\theta}$  replaced by a column vector  $\begin{bmatrix} \dot{\theta} \\ \underline{v} \end{bmatrix}$ .

An external electric field breaks parity symmetry and, in three dimensions, makes visible [10] in the laboratory frame cross-correlations such as  $\langle \underline{v}(t) \underline{\omega}^T(0) \rangle$  where  $\underline{\omega}$  is the usual three-dimensional molecular angular velocity.

Assuming that these cross-correlations still exist when the dimensionality of the system is reduced from three to two, then it follows that equation (3) is an incomplete description of the system under consideration and must be extended to include the electric field induced roto-translational cross-correlations. A convenient way of doing this is to rewrite equation (3) as:

$$I\ddot{\theta} + I(\beta - i\omega_1)\dot{\theta} + V'_1(\theta) + \mu E \sin \theta = \dot{W}(t) \quad (4)$$

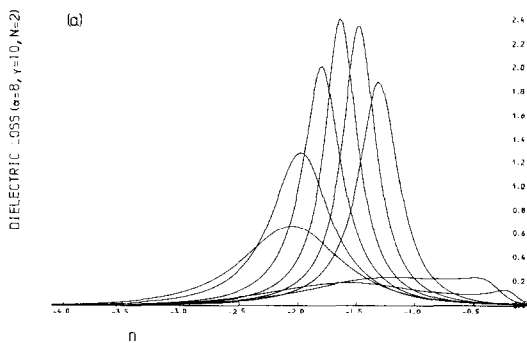
with the assumption that  $\omega_1 = 0$  for  $E = 0$ , i.e.  $Ii\omega_1\dot{\theta}$  is a

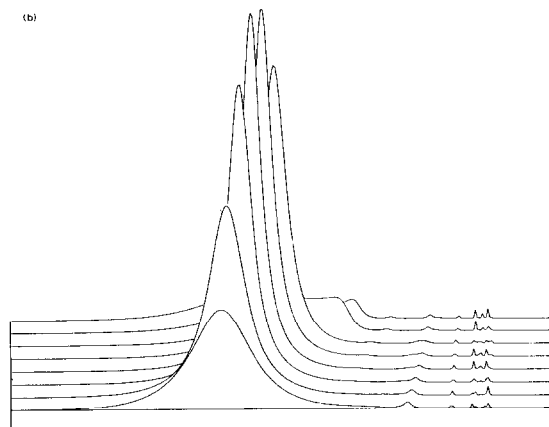
term whose effect is to introduce dynamical cross-correlations in response to an electric field  $\underline{E}$  applied externally to the sample. Equation (5) can be solved straight-forwardly with the numerical differential-difference algorithm described by Reid [1], using complex arithmetic in the computer. This paper reports the solution of equation (4) by varying  $\omega_1$  for constant  $\alpha, \beta, \gamma$ , and  $N$

## RESULTS

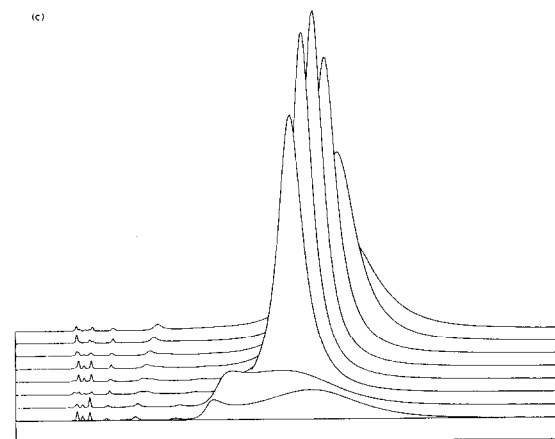
The solution of equation (4) for  $\alpha(\omega)$  and  $\epsilon''(\omega)$  follows the method of Reid. The complex arithmetic was evaluated with FORTRAN complex arithmetic of the CDC 7600 computer. The real part of  $\epsilon''(\omega)$  shows a series of cycles as  $\omega_1$  is increased. The first of these is illustrated in Fig (1) for the low frequency part of the overall loss profile. The 3-D schematics of Fig 1(b) and Fig. 1(c) shows the complete range of  $\epsilon''(\omega)$ , including the far infra-red. (For computational convenience in these curves, the angle between  $\underline{\mu}$  and  $\underline{E}$  has been set at  $2\theta$ , and the well multiplicity  $N$  has also been taken as  $N = 2$ , thus eliminating cross-coefficients in the differential-difference matrix inversion technique by Reid [1]. Most of the features of the solution to equation (3) reported below are expected to persist in the presence of cross-terms,  $V_1(\theta)$  in equation (3).) The reversed view of Fig. 1(c) illustrates the particularly interesting

R ( $\beta$ ) = 0.1, -ln ( $\beta$ ) = .1, .2, .3, .4, .5, .6, .9, 1





3-D PLOTS OF DIELECTRIC LOSS SHOWING THE FIRST CYCLE  
 FROM THE FRONT,  $\text{IM}(\epsilon_2) = 0.1, 0.2, 0.3, 0.4, 0.5, 0.6, 0.9, 1.0$



3-D PLOTS OF DIELECTRIC LOSS SHOWING THE FIRST CYCLE  
 FROM THE BACK,  $\text{IM}(\epsilon_2) = 0.1, 0.2, 0.3, 0.4, 0.5, 0.6, 0.9, 1.0$

### Figure (1)

- (a) The first cycle in  $\epsilon''(\omega)$  as function of  $\omega_1$ . The abscissa is  $\log_{10}(\omega) - 12$ . Far infra-red fine structure not shown.
- (b) Schematic of fig. 1(a), showing peaks in the first part of the 1st cycle, plus far infra-red detail.
- (c) Back view of fig. 1(b), showing reverse frequency dependence of loss peaks in the latter part of the first cycle.

behaviour at the end of the first cycle ( $\omega_1 = 0.9\text{THz}$  and  $\omega_1 = 1.0\text{THz}$ ) where the main dielectric loss breaks into two peaks and becomes broader than the Debye half-width of 1.12 decades. The behaviour of the loss curve in this region is detailed further in Fig. (2). As  $\omega_1$  is increased further the sequence of dielectric loss curves  $\epsilon''(\omega)$  goes into a second cycle, whose component curves are sharper and more intense than those of cycle 1. The second cycle occupies the range  $1.0\text{ THz} < \omega_1 < 4.0\text{ THz}$ . At about 4.0 THz a secondary lower frequency loss process appears again which is broader than in the first cycle, and peaks at a slightly lower  $\omega$ . The whole process then goes into a third and more cycles for  $\omega_1 > 4.0\text{ THz}$ . At the same time, the equivalent process in terms of the far infra-red power absorption coefficient causes the numerous peaks in  $\alpha(\omega)$  to change in relative intensity and frequency, as reported experimentally [7,8]. The whole of this process takes place in the low friction (or barrier crossing-frequency) limit ( $\beta = 0.1\text{ THz}$ ) for fixed values of  $\alpha = 8.0\text{ THz}$  and  $\gamma = 10\text{ THz}$ .

ELECTRIC FIELD EFFECTS (REAL  $\beta$ ) = 0.1)

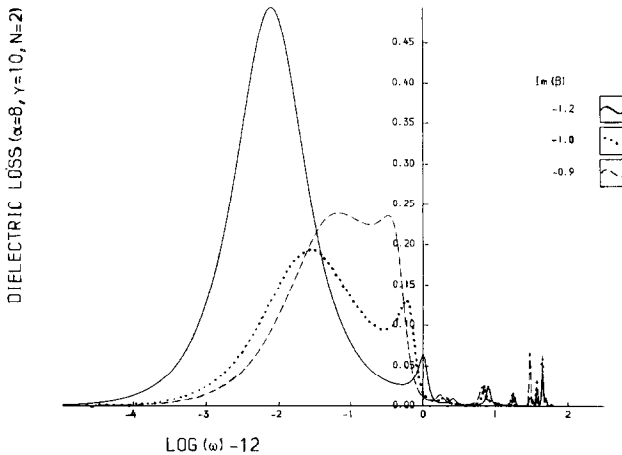


**Figure (2)**

Behaviour of  $\epsilon''(\omega)$  towards the end of the first cycle, ( $\omega_1 = 0.9\text{ THz}$ ,  $\omega_1 = 1.0\text{ THz}$ ,  $\omega_1 = 1.2\text{ THz}$ ).

It is worth noting that  $\omega_1 = 1.0$  THz and  $I = 10^{-40}$  gm cm<sup>2</sup> correspond to an electric field strength of 100 volts cm<sup>-1</sup> for a dipole moment  $\mu = 1.0D$ . It is interesting to note also that the same type of equations as used here for the molecular dynamical processes responsible for  $\epsilon''(\omega)$  and  $\alpha(\omega)$  can be used in several related areas of investigation as emphasised by Grigolini et al [6], and by Reid [1]. One of the most important of these is superconductivity and Josephson junction V-I characteristics and hysteresis, whose equations are formally identical with eqns (1)-(3) with  $\omega_1 = 0$ . The appearance of peaks in the low friction limit should have interesting physical analogies in these related areas of research, especially in the presence of alternating or circularly polarised external fields.

### DISCUSSION

The effective potential in the presence of an external electric field is:

$$V(\theta) = -V_0 \cos(N(\theta - \theta_0)) - \mu E \cos \theta.$$

Let us assume however, for the sake of simplicity, that

$$\ddot{\theta} + (\beta - i\omega_1) \dot{\theta} + \frac{V_0(E)}{I} \sin \theta = \frac{f(t)}{I} = F(t) \quad (5)$$

where  $V_0(E) = V_0 + \mu E$  and  $F(t)$  is a Gaussian white noise with zero mean-value.

When  $\omega_1 = 0$  the fluctuation dissipation relation is assumed ( $\langle \theta^2 \rangle_{eq} = kT/I$ )

$$\langle f(t)f_0 \rangle = 2D\delta(t) \quad (6)$$

$$\begin{aligned} D &= I^2\beta \langle \theta^2 \rangle_{eq} \\ &= I\beta kT. \end{aligned}$$

Introducing a complex friction constant means that  $F(t)$  must be split into two statistically related components:

$$\begin{aligned} F(t) &= F_x(t) + i F_y(t) \\ &= \frac{f_R(t)}{I} + \frac{if_I(t)}{I} \end{aligned} \quad (7)$$

so that

$$\langle f_R(t) f_R(0) \rangle = 2D_{RR} \delta(t) \quad (8)$$

$$\langle f_I(t) f_I(0) \rangle = 2D_{II} \delta(t) \quad (9)$$

$$\langle f_R(t) f_I(0) \rangle = D_{RI} \delta(t) \quad (10)$$

$$D_{RI} = D_{IR}$$

By applying, formally, the fluctuation dissipation theorem we find:

$$D_{RR} - D_{II} = \beta \frac{kT}{I} \quad (11)$$

$$D_{RI} = D_{IR} = -\omega_1 \frac{kT}{I} \quad (12)$$

In general,  $\theta(t)$  is now a complex variable:

$$\theta(t) = x(t) + iy(t), \quad (13)$$

so that:

$$\frac{d}{d\theta} \rightarrow \frac{d}{dx} - i \frac{d}{dy}. \quad (14)$$

Eqn (5), for a complex  $\theta(t)$ , can be rewritten as:

$$\left. \begin{aligned} \ddot{x} + \beta \dot{x} + \omega_1 \dot{y} + \frac{d}{dx} V(x,y) &= F_x(t) \\ \ddot{y} + \beta \dot{y} - \omega_1 \dot{x} - \frac{d}{dy} V(x,y) &= F_y(t) \end{aligned} \right\} \quad (15)$$

where

$$V(x,y) = -\frac{V_0(E)}{I} \cos x \cosh y \quad (16)$$

This is a pseudo-potential, formally valid for the problem at hand, but which cannot be recovered from the set of standard canonical equations obtained from the relevant Louvillian Equation (15) can be written as

$$\ddot{\underline{X}} + \underline{\Gamma} \dot{\underline{X}} + \nabla V(x,y) = \underline{F} \quad (17)$$

where

$$\underline{X} = \begin{bmatrix} x \\ y \end{bmatrix}, \quad \underline{\Gamma} = \begin{bmatrix} \beta & \omega_1 \\ -\omega_1 & \beta \end{bmatrix};$$



$$\underline{\nabla} = \begin{bmatrix} d/dx \\ -d/dy \end{bmatrix}; \quad \text{and} \quad \underline{F}(t) = \begin{bmatrix} F_x(t) \\ F_y(t) \end{bmatrix}$$

with

$$\langle F_x(t) F_x(0) \rangle = 2D_{xx} \delta(t)$$

$$\langle F_y(t) F_y(0) \rangle = 2D_{yy} \delta(t)$$

$$D_{xx} = I^2 \beta \langle \dot{x}^2 \rangle$$

$$D_{yy} = I^2 \beta \langle \dot{y}^2 \rangle$$

$$\langle F_x(t) F_y(0) \rangle = D_{xy} \delta(t)$$

$$D_{xy} = D_{yx} = -\omega_1 I \beta kT$$

$$I^2 \beta (\langle \dot{x}^2 \rangle - \langle \dot{y}^2 \rangle) = I \beta kT$$

for consistency with eqns (11) and (12).

#### PHYSICAL INTERPRETATION OF EQUATION (15)

It is assumed that an external field  $\underline{E}$  triggers rotation/translation coupling in the laboratory frame by breaking the parity inversion symmetry of the overall hamiltonian. In particular it is assumed that  $\omega_1$  depends on  $E$ , so that

$$\omega_1(E = 0) = 0 \quad (18)$$

In the limit  $E \rightarrow 0$  the two equations (15) decouple, into purely rotational and translational Langevin equations. In this limit

$$x \rightarrow \theta \quad \text{and} \quad \lim_{E \rightarrow 0} V(x, y) = V(\theta) \quad (19)$$

with  $V(\theta)$  as used in equation (2). The variable  $y$  of equation (15) must be dimensionless. The only quantity relevant to the problem having dimensions of the inverse of length is  $e_0 E / (kT)$ , where the  $e_0$  charge is defined microscopically by

$$e_0 = \frac{|\underline{\mu}|}{|a|} \quad (20)$$

where  $a$  is an intrinsic length scale (of the order of the spacing between rotators or diameter of the rotator itself for example), so that

$$r_0(E) = \left[ \frac{\mu E}{kT} \right]^{-1} a \quad \text{and}$$

$$Y \rightarrow \frac{r}{r_0(E)} \quad (21)$$

The potential  $V(x, y)$  can then be rewritten as:

$$- V_0(E) \cos \theta \cosh (r/r_0(E)) \quad (22)$$

with:

$$\langle \dot{\theta} \rangle = \left[ \frac{\mu E}{kT} \right]^2 \frac{\langle V^2 \rangle}{a^2} + \frac{kT}{I} \quad , \quad (23)$$

the mean square linear, centre of mass velocity  $\langle V^2 \rangle$  being  $kT/m$ , and the mean square rotational velocity:

$$\langle \dot{\theta}^2 \rangle = \left[ \frac{\mu E}{kT} \right]^2 \frac{kT}{ma^2} + \frac{kT}{I} \quad (24)$$

Equation (17) now becomes:

$$\begin{aligned} \underline{\dot{X}} &= \begin{bmatrix} \dot{\theta} \\ \dot{r} \end{bmatrix} ; \quad \underline{\Gamma} = \begin{bmatrix} \beta & \omega_1/r_0 \\ -\omega_1 r_0 & \beta \end{bmatrix} ; \\ \underline{\dot{Y}} &= \begin{bmatrix} d/dx \\ r_0^2 d/dy \end{bmatrix} ; \quad \text{and} \quad \underline{F}(t) = \begin{bmatrix} F_x(t) \\ r_0 F_y(t) \end{bmatrix} \end{aligned} \quad (25)$$

The displacement  $\underline{r}$  can be thought of as the displacement of the tagged polar molecule from the centre of the annulus (surrounding cage of molecules) generating the multiwell potential and mimicking the "spectator" cage.

The presence of the potential (22) presents large displacements  $|\underline{r}|$  from taking place because of the presence of the external electric field  $\underline{E}$ . When there is no external electric field there is no restraint on  $\underline{r}$ . This means that the electric field tends to line up the dipole moments  $\underline{\mu}$  of the individual molecules in the sample. The rate at which the dipoles line up is dependent in the same way on  $\mu E/kT$ . This implies that any displacement of the tagged molecule from its minimum potential energy site would bring aligned dipole-moments closer together, the resultant repulsion justifying the confining potential term  $\cosh \left[ \frac{\mu E}{kT} \frac{r}{a} \right]$ .

In other words the action of an electric field  $\underline{E}$  makes the tagged molecule sense the presence of the remaining dipoles and therefore introduces a type of finite-range correlation

$\left[ r_0(E) \rightarrow \infty \right]_{E \rightarrow 0}$ . It is possible to extend this interpretation to three-dimensions using:

$$Y = \frac{\mu E - \tau}{kTa}$$

but the two dimensional interpretation used above is simpler.

Finally, the multiplicative coupling

$$\cos \theta \cosh (r/r_0(E))$$

can be justified by assuming that when  $r \neq 0$  the tagged molecule is closer to the annulus (cage) and therefore the coupling with it is stronger.

This type of potential is therefore the result of using a "complex friction" in the Kramers equation. The real part of this "complex friction" is the Kramers barrier-crossing rate. When this is low, the far infra-red spectrum splits into the numerous separate peaks described in this paper.

#### ACKNOWLEDGEMENTS

The University of Wales is thanked for a Fellowship, and the Nuffield Foundation for a bursary.

#### REFERENCES

1. C.J. REID, Mol. Phys., 49 (1983) 331.
2. H.A. KRAMERS, Physica, 7 (1940) 284.
3. W.T. COFFEY, M.W. EVANS, and P. GRIGOLINI, "Molecular Diffusion", Wiley/Interscience, N.Y., 1984, Chapters 3-6.
4. M.W. EVANS, G.J. EVANS, W.T. COFFEY and P. GRIGOLINI, "Molecular Dynamics", Wiley/Interscience, N.Y., 1982, Chapter 7.
5. Z. SCHUSS, "Theory and Applications of Stochastic Differential Equations", J. Wiley & Sons, N.Y. (1980).

6. "Memory Function Approach to Stochastic Problems in Condensed Matter", Special Issue of "Advances in Chemical Physics", Ed. M.W. Evans, P. Grigolini, and G. Pastori-Parravicini, Wiley/Interscience N.Y., gen. ed., Prigogine, and Rice, vols. 62 and 63, (1985).
7. G.J. EVANS, and M.W. EVANS, J. Chem. Soc., Faraday Trans: II. 79 (1983) 547.
8. G.J. EVANS and M.W. EVANS, J. Chem. Soc., Chem. Commun., 1978, p. 267.
9. Ref. (4), Chapter 5.
10. M.W. EVANS and G.J. EVANS, Phys. Rev. Letters., 53 (1985) 818; Phys. Lett., 103A (1984) 323.
11. Ref. (4), Introductory Chapter.